Epithelial reticulon 4B (Nogo-B) is an endogenous regulator of Th2-driven lung inflammation

Paulette L. Wright,[1] Jun Yu,[1] Y.P. Peter Di,[3] Robert J. Homer,[4] Geoffrey Chupp,[2] Jack A. Elias,[2] Lauren Cohn,[2] and William C. Sessa[1]

[1]Vascular Biology and Therapeutics Program, Departments of Pharmacology and Medicine, and [2]Section of Pulmonary and Critical Care Medicine, Department of Internal Medicine, Yale School of Medicine, New Haven, CT 06510
[3]Department of Environmental and Occupational Health, Graduate School of Public Health, University of Pittsburgh, Pittsburgh, PA 15219
[4]Department of Pathology, Yale School of Medicine and Pathology and Laboratory Medicine Service, VA CT HealthCare System, West Haven, CT 06516

Nogo-B is a member of the reticulon family of proteins (RTN-4B) that is highly expressed in lung tissue; however, its function remains unknown. We show that mice with Th2-driven lung inflammation results in a loss of Nogo expression in airway epithelium and smooth muscle compared with nonallergic mice, a finding which is replicated in severe human asthma. Mice lacking Nogo-A/B (Nogo-KO) display an exaggerated asthma-like phenotype, and epithelial reconstitution of Nogo-B in transgenic mice blunts Th2-mediated lung inflammation. Microarray analysis of lungs from Nogo-KO mice reveals a marked reduction in palate lung and nasal clone (PLUNC) gene expression, and the levels of PLUNC are enhanced in epithelial Nogo-B transgenic mice. Finally, transgenic expression of PLUNC into Nogo-KO mice rescues the enhanced asthmatic-like responsiveness in these KO mice. These data identify Nogo-B as a novel protective gene expressed in lung epithelia, and its expression regulates the levels of the antibacterial antiinflammatory protein PLUNC.

CORRESPONDENCE
William C. Sessa:
william.sessa@yale.edu

Abbreviations used: BAL, bronchioalveolar lavage; BMT, BM transplantation; CCSP, Clara cell secretory protein; DTG, double transgenic; HA, hemagglutinin; NHBEC, normal human bronchial epithelial cell; PAS, periodic acid-Shiff; PLUNC, palate lung and nasal clone; RTN, reticulon; SMA, smooth muscle actin.

The reticulon (RTN) family of proteins in mammals is composed of four members, RTN-1, -2, -3, and -4, which have been characterized by the presence of a highly conserved RTN homology domain in their C-terminal end, which is thought to be important for their localization in the ER (Oertle and Schwab, 2003; Woolf, 2003). While in the ER, RTNs are postulated to serve fundamental cell-autonomous roles in shaping and structuring ER membranes; however, because yeast and mice lacking various RTNs are viable, they are not essential for cell survival, possibly because of compensatory mechanisms to preserve ER integrity (Voeltz et al., 2006; Shibata et al., 2008). Recent studies have shown functions for RTNs under conditions of stress or injury, suggesting that they exert permissive roles to enhance or reduce stressful insults (Teng and Tang, 2008). Evidence for this has been elucidated for RTN-4A and RTN-4B (also called Nogo-A and –B), the most well studied of the mammalian RTN family of proteins (Chen et al., 2000; GrandPré et al., 2000; Prinjha et al., 2000; Acevedo et al., 2004; Fontoura et al., 2004; Rodriguez-Feo et al., 2007; Kritz et al., 2008; Yu et al., 2009).

RTN-4 or the Nogo family is encoded by a single gene with three major isoforms, Nogo-A, -B, and -C, which are generated by alternative splicing for Nogo-A and -B and by alternative promoter utilization for Nogo-C (Oertle and Schwab, 2003). Nogo-A and -C are primarily distributed in the CNS, with Nogo-C additionally expressed in skeletal muscle, whereas Nogo-B is more ubiquitously expressed in a variety of tissues and cells in culture (Oertle and Schwab, 2003). Nogo-A, the largest of the Nogo isoforms, was first identified as a myelin-associated inhibitor of axon regeneration and neurite outgrowth after CNS injury (Chen et al., 2000; GrandPré et al., 2000; Prinjha et al., 2000). Other studies have

The Rockefeller University Press $30.00
J. Exp. Med. Vol. 207 No. 12 2595-2607
www.jem.org/cgi/doi/10.1084/jem.20100786

identified a potential role for Nogo-A in pathogenesis of experimental autoimmune encephalomyelitis, an animal model of human multiple sclerosis (Fontoura et al., 2004). The Nogo-B isoform is highly expressed in vascular smooth muscle cells, endothelial cells, and monocytes/macrophages, and in the context of the vasculature, the loss of Nogo promotes vascular injury (Acevedo et al., 2004; Kritz et al., 2008; Yu et al., 2009). Therapeutic delivery of Nogo-B in both murine and porcine models of acute vascular injury reduces the extent of vascular growth and neointima formation (Kritz et al., 2008). In humans, Nogo-B levels are reduced in atherosclerotic tissue and aortic aneurysms, and this reduction may contribute to plaque formation, destabilization, and vascular abnormalities (Pan et al., 2007; Rodriguez-Feo et al., 2007). However, little is known about the in vivo expression of Nogo-B or its function outside the vasculature.

In the present work, we show that Nogo-B is highly expressed in mouse and human lung tissue, most strikingly in pulmonary airways. During allergic asthma-like inflammation in the lung, the levels of Nogo-B in epithelia and bronchiolar smooth muscle are reduced and the genetic loss of Nogo augments lung inflammation in a mouse model of antigen-driven Th2 inflammation. Transgenic expression of Nogo-B in pulmonary epithelium reduces asthma-like inflammation via the expression of palate lung and nasal clone (PLUNC), an antiinflammatory protein exclusively expressed in the nasal cavity and upper airways. Thus, Nogo-B in epithelial cells is a newly described regulator of the extent of allergic Th2 lung inflammation.

RESULTS

Nogo-B is highly expressed in the lung

To examine Nogo gene expression in vivo, mice harboring a LacZ reporter inserted into the Nogo gene locus (Nogo-A/B$^{+/-}$ mice) were used (Kim et al., 2003). Remarkably, Nogo-A/B gene expression is highly expressed in the lung (Fig. 1 A). As seen in Fig. 1 B (top), Nogo is expressed in airways (Fig. 1 B, labeled A) both in E-cadherin–positive epithelium and smooth muscle actin (SMA)–positive airway smooth muscle and blood vessels (Fig. 1 B, labeled V). The same pattern of Nogo protein expression was confirmed by immunohistochemical staining of C57BL6 WT lung sections with a Nogo-A/B–specific antibody (Fig. 1 B, bottom), using lung sections from Nogo-A/B$^{-/-}$ mice to verify specificity of the Nogo-A/B antibody (Fig. 1 B, inset). Because Nogo-A/B$^{-/-}$ mice lack both Nogo-A and –B, whole lung lysates were analyzed for relative levels of these isoforms (using brain as a control for Nogo-A and lysates from heart or lung endothelial cells for Nogo-B). As seen in Fig. 1 C, Nogo-B is the predominant isoform in the lung as Nogo-A was undetectable. Therefore, Nogo function in the lung is most likely attributable to the Nogo-B isoform.

Expression of Nogo is reduced in a mouse model of antigen-driven Th2 inflammation and in human severe asthma

To investigate if Nogo expression changes in the lung during asthma pathogenesis, we used the well established OVA model of antigen-driven Th2-dependent acute allergic inflammation that generates an asthma-like response in mice (Wang et al., 2000). Initially, changes in total lung Nogo-B protein were evaluated by comparing levels in control versus allergic lungs in WT mice sensitized with OVA plus alum and subsequently challenged with aerosolized OVA (allergic mice) or PBS only (nonallergic mice). Allergic mice developed a modest decrease in total lung Nogo-B protein levels as compared with nonallergic mice (Fig. 2 A). Both PBS treatment and OVA challenge without prior sensitization or, conversely, sensitization without aerosolized OVA challenge did not induce Nogo-A or alter Nogo-B protein levels (Fig. S1). Next, alterations in cell type–specific Nogo protein levels were evaluated in WT mice via immunostaining with a Nogo-A/B antibody. Interestingly, the levels of immunoreactive Nogo protein decreased in airway epithelial and smooth muscle cells in allergic lungs (Fig. 2 B, c and d, arrowheads) but remained in vessels (Fig. 2 B, b–d, asterisks), whereas Nogo levels were unchanged in nonallergic lungs (Fig. 2 B, a and b, arrowheads). Quantification of immunoreactive Nogo levels demonstrated a marked reduction in the epithelium and smooth muscle of the airways in allergic lungs (Fig. 2 B, graphs). To address whether the loss of Nogo reflected changes in integrity of the epithelial layer (such as sloughing of the epithelium) or in epithelial morphogenesis (such as goblet cell hyperplasia), serial sections of airways were stained, respectively, with E-cadherin to delineate the epithelium lining or periodic acid-Shiff (PAS) which stains for mucus (Fig. 2 B, e and f, and i and j, respectively). However, there was no correlation between decreases in Nogo levels, compromised integrity of the epithelium, or morphological changes. To determine if changes in Nogo levels in asthma-like mouse lungs extrapolates to human tissue, we evaluated immunoreactive Nogo levels in normal and fatal asthmatic lung specimens. Immunoreactive Nogo was present at high levels throughout the lung, with particular expression noted in the airway epithelium, smooth muscle, and vasculature (Fig. 2 C, a and c). Similar to findings in the mouse, there was a marked reduction in Nogo levels in epithelium and smooth muscle of asthmatic specimens (Fig. 2 C, b and d, arrowheads). These results were repeated in an additional normal specimen and three additional asthmatic specimens (Fig. S2).

To explore whether the reduction in Nogo protein levels in large and moderate airway epithelia and smooth muscle was a result of changes in Nogo gene expression, Nogo-A/B LacZ gene reporter mice were OVA sensitized and challenged and lung sections were stained with X-gal. OVA challenge reduces Nogo gene expression in airway epithelium that mimics the protein changes observed in allergic lungs (Fig. 2 D). In contrast, Nogo gene expression is enhanced in the vasculature throughout the lung in allergic mice, which was not obvious at the protein level as a result of sensitivity limitations of the immunostaining. Sections were also counterstained with E-cadherin or SMA to ensure the presence of the epithelium and to distinguish airways and vessels. These data clearly show that Nogo gene and protein expression in the lung is altered during settings of acute allergic asthma-like responses and in

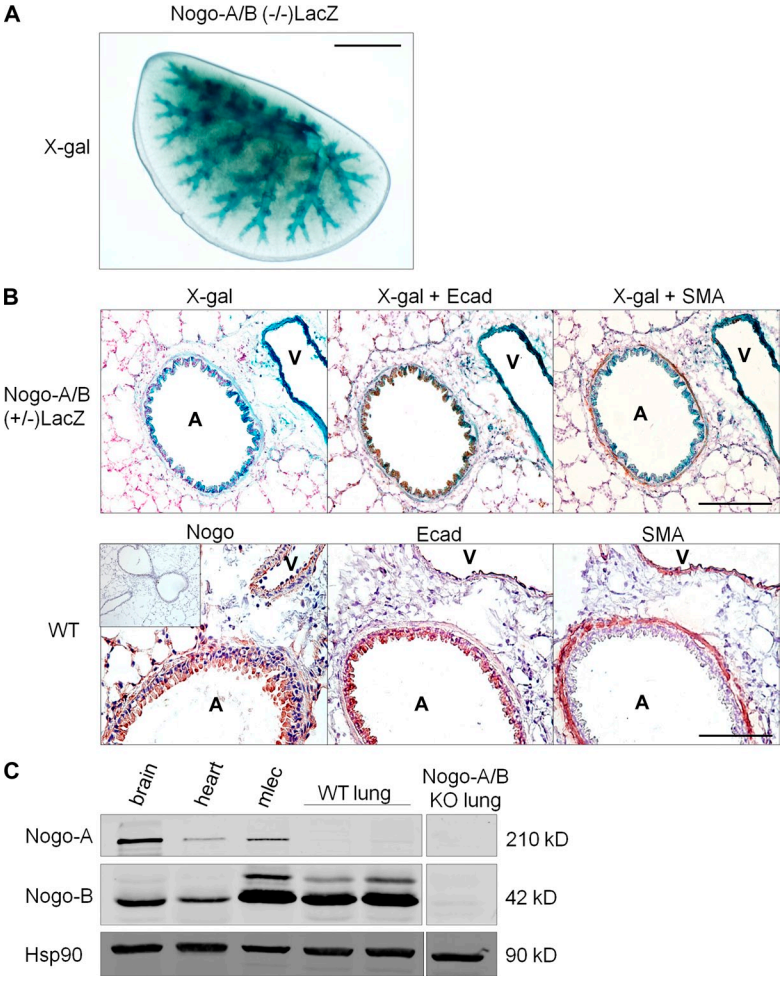

Figure 1. Nogo-B is highly expressed in the lung. (A) Whole-mount X-gal staining of Nogo-A/B KO LacZ mouse lung tissue. Blue indicates positive Nogo-A/B gene expression throughout the lobe. Bar, 0.5 mm. (B) X-gal–stained lung sections from Nogo-A/B$^{+/-}$ LacZ mice (top). Blue indicates positive Nogo gene expression in epithelium and smooth muscle of airways (A), and endothelial and smooth muscle cells of vessels (V), as well as parenchymal cells. Also shown are lung sections from WT mice stained with Nogo-A/B antibody 1761 (bottom). Brown staining indicates positive Nogo protein expression, and specificity of antibody was confirmed with negative staining of Nogo-A/B KO lung section (inset). Sections were also labeled with anti–E cadherin (Ecad) or α-SMA to delineate epithelium and smooth muscle, respectively. Bars: (top) 200 µm; (bottom) 100 µm. (C) Lysates were immunoblotted with a Nogo-A/B antibody. Brain lysate is as a positive control for Nogo-A. Heart and mouse lung endothelial cells (mlecs) are positive controls for Nogo-B. Lung lysate from Nogo-A/B KO mice is a negative control and hsp90 is a loading control.

a human asthmatic, and Nogo expression is affected differentially in airways and vessels.

Nogo-A/B$^{-/-}$ mice display enhanced asthma-like responses

To determine whether endogenous Nogo promotes or limits lung inflammation, WT and congenic Nogo-A/B$^{-/-}$ mice (herein referred to as KO; Zheng et al., 2003) were OVA sensitized and challenged. Under baseline conditions, lungs from nonallergic KO mice were virtually identical to WT mice as indexed by lung histology and the absence of mucus staining by PAS. However, lungs from allergic KO mice had increased levels of inflammatory cells, mucus production (Fig. 3 A; top and bottom), and indices of airway hyperreactivity (Fig. S3) compared with WT mice. To determine the extent of lung inflammation and cellular composition, bronchioalveolar lavage (BAL) fluid was collected and evaluated for total and differential cell counts. OVA-sensitized and challenged KO mice display a 60% increase in total cell infiltrates, which are predominantly eosinophils, whereas macrophages, lymphocytes, and neutrophils were comparable in number between WT and KO mice (Fig. 3 B). The increase in inflammation in KO mice was associated with higher levels of Th2 cytokines in BAL (IL-13, IL-4, and IL-5), whereas IFN-γ (a typical Th1 cytokine) was almost undetectable in BAL of both strains (Fig. 3 C). IgE levels were also analyzed in mice before and after aerosolized OVA challenge. Blood total IgE (not depicted) and OVA-specific IgE levels were identical in WT and KO mice after sensitization but before challenge; however, after the third aerosolized OVA challenge, OVA-specific IgE levels were elevated in KO mice (Fig. 3 D), suggesting that mice lacking Nogo-A/B have dysregulated effector responses in this model of antigen-driven Th2 inflammation.

To help address the temporal aspects of the role of Nogo limiting inflammation in this model, BAL cellularity was examined 24 h after a single challenge rather than after a 3-d challenge. Lung inflammation is significantly elevated in KO mice 24 h after a single challenge of aerosolized OVA as compared with WT (Fig. 3 E, total cells and eosinophils). Additionally, to determine effects of Nogo on the resolution of lung inflammation, BAL cellularity was evaluated in mice 7 and 14 d after challenge. KO mice displayed enhanced inflammation that persists at least out to 7 d, compared with WT mice, and the inflammatory response in all mice was resolved by 14 d (Fig. 3 F); however, a few residual eosinophils were present in KO mice at the latest time point. Finally, to examine if Nogo is important for Th1 lung inflammation, WT and KO mice were sensitized with CFA/OVA and then challenged with aerosolized OVA as described in Materials and methods. The loss of Nogo did not influence CFA-induced lung inflammation (Fig. S4).

Loss of Nogo-A/B in resident lung cells is responsible for enhanced asthma-like inflammation

Because Nogo-B is expressed in many cell types in the lung and inflammatory cells, we examined its function in the resident lung tissue (i.e., the structural cells) versus inflammatory cells via BM transplantation (BMT) experiments. BMT was

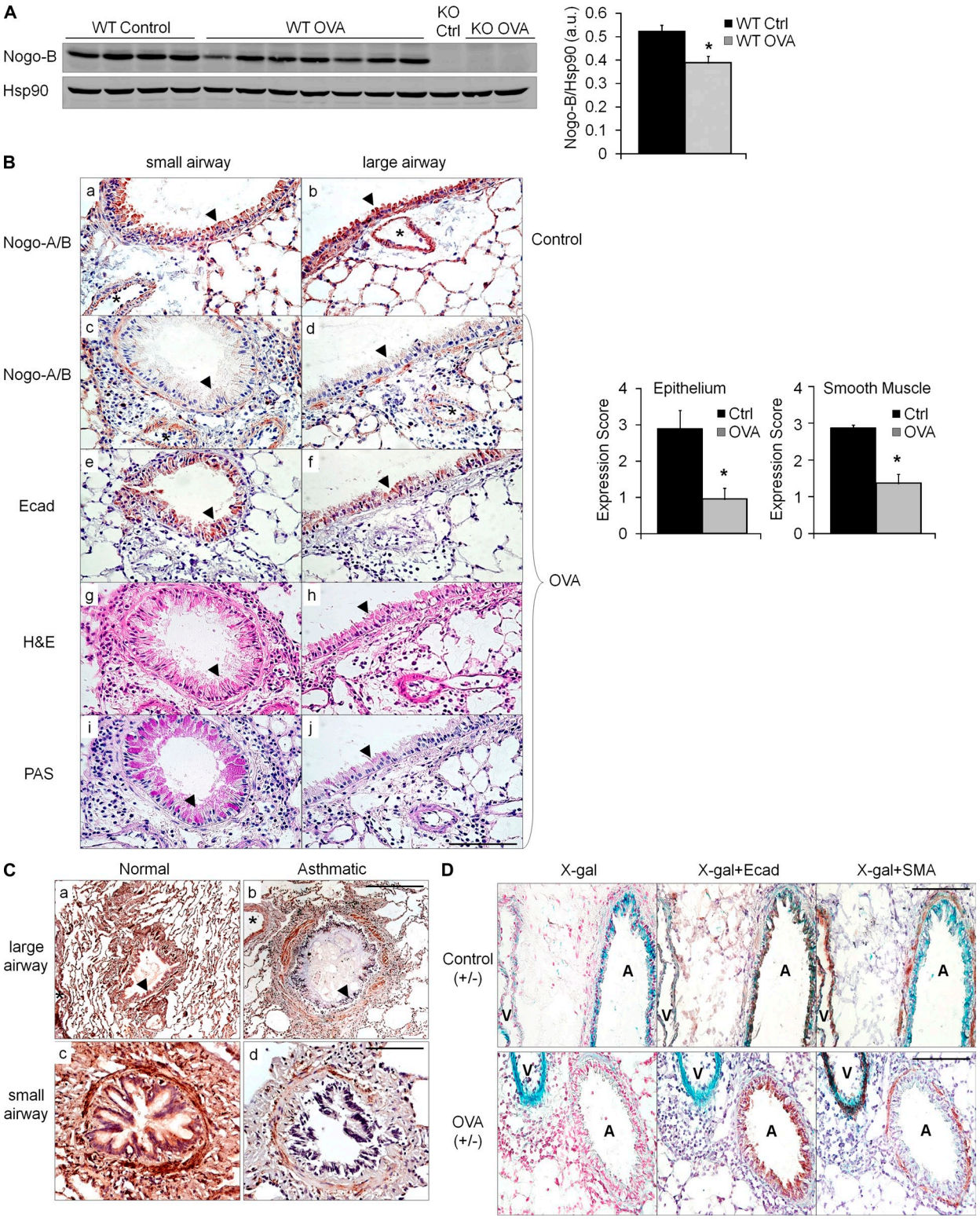

Figure 2. Regulation of Nogo-B expression during asthma-like conditions in mice and human asthma. (A) Nogo-B protein levels were significantly decreased in total lung lysates of OVA-sensitized and challenged (allergic) mice versus WT control (nonallergic) mice. Shown is a typical Western blot from six individual experiments. Nogo-B levels were quantified by densitometry and normalized to hsp90 (*, $P < 0.05$). Data are expressed as mean ± SEM. $n = 4–7$ mice per group. (B) Lung sections from representative small and large airways of untreated (control, a and b) and OVA-challenged (c and d) WT mice stained with Nogo-A/B antibody. Brown indicates positive Nogo-A/B in airway epithelium (arrowheads), smooth muscle and vessels (asterisk) of control mice, and the loss of Nogo immunoreactivity in epithelium and smooth muscle, but not vessels (*, c and d), of OVA-challenged mice. Bar, 100 µm.

conducted by transferring BM from WT and KO mice into 8-wk-old lethally irradiated KO and WT mice, respectively, as well as matching genotypes for controls, and allowing reconstitution for 8 wk. Mice were then OVA-sensitized and challenged as described and analyzed for levels of inflammation. Consistent with initial observations, KO BM transplanted into KO mice displayed enhanced asthma-like inflammation as compared with WT BM cells transplanted into WT mice (Fig. 3, G and H), whereas KO BM transplanted into WT mice resulted in similar levels of Th2 inflammation, as observed in WT mice with WT BM. In contrast, WT BM transplanted into KO mice resulted in a marked increase in allergic inflammation similar to levels found in KO mice transplanted with KO BM. Therefore, these data suggest that Nogo is acting predominantly within the structural cells resident in the host lung tissue to attenuate asthma-like inflammation.

Transgenic Nogo-B expression in lung epithelium attenuates asthma-like inflammation

To examine whether the loss of Nogo-B in epithelial cells influences the extent of allergic Th2 responses, tetracycline (TET)-inducible cell-specific Nogo-B transgenic mice were generated via breeding a pTet splice–TRE-hNogo-B-hemagglutinin (HA)–tagged mouse to a (TET-ON) Clara cell secretory protein (CCSP) promoter driver line (Tichelaar et al., 2000) to create CCSP-Nogo-B double transgenic (DTG) mice. DTG mice were put on doxycycline over several days and evaluated for expression of the transgene. Nogo-B HA is expressed in a time-dependent manner with a maximum expression after 7 d in lung lysates (Fig. 4 A) and the transgene localizes to the large airway epithelium (Fig. 4 B). Because these mice were used exclusively as an ON system, STG mice served as a control group for subsequent experiments.

Next, we tested whether transgenic expression of Nogo-B into the airway epithelium would rescue the loss of Nogo after OVA challenge and/or alter the extent of asthma-like inflammation. Both STG and DTG mice were placed on doxycycline water for 2 wk before OVA sensitization to stabilize transgene expression. Mice were then subjected to OVA sensitization and challenge and evaluated for allergic asthma-like response parameters. First, proper induction of Nogo-B transgene expression was established with the presence of HA-tagged transgene in airway epithelium of nonallergic DTG lungs (Fig. 4 C, b, arrowhead), which was absent in nonallergic STG lungs (Fig. 4 C, a, arrowhead). Importantly, Nogo-B transgene expression was preserved in the airway epithelium of allergic lungs (Fig. 4 C, d, arrowhead), whereas endogenous Nogo-B is decreased in airway epithelium of STG-allergic lungs (Fig. 4 C, e, arrowhead), which is consistent with observations in WT allergic mice. This implies that the asthmatic-like milieu is responsible for the loss of endogenous airway epithelial Nogo gene expression, yet it is not sufficient to affect Nogo-B transgene expression which is under the control of the CCSP promoter. Allergic DTG mice displayed a marked reduction in total inflammatory cells in the tissue (Fig. 4 C, h) and BAL (Fig. 4 D), which was mainly reflective of eosinophil levels as compared with STG-allergic mice (Fig. 4, C [g] and D, respectively). Allergic DTG mice also generated lower levels of Th2 cytokines in their BAL, including IL-13, IL-4, and IL-5 (Fig. 4 E), as well as lower levels of mucus production compared with allergic STG mice (Fig. 4 C, j and i, respectively), which is indicative of a reduced asthmatic response. In contrast, mice that inducibly express Nogo-B in vascular endothelium using an endothelial-specific (VE-cadherin) Tet-regulated driver line displayed no differences in asthma-like responses as compared with control mice (unpublished data). To exclusively conclude that Nogo-B in epithelium is functioning in the DTG mice during the effector phase of the response, adoptive transfer of OTII $CD4^+$ Th2 cells into STG and DTG mice was conducted, followed by OVA challenge via aerosolization. DTG mice displayed an attenuated inflammatory response (in total BAL and lung histology) compared with STG (Fig. 4 F). Collectively, these data show that transgenic replacement of Nogo-B into the lung epithelium during allergic Th2 inflammation attenuates the effector phase of this response.

Genome-wide arrays demonstrate that endogenous Nogo-B regulates the expression of the PLUNC gene

To help decipher a mechanism for how Nogo functions in the lung, a genome-wide microarray of naive WT and KO lungs was conducted. Among 40,000 genes investigated, only one gene other than Nogo-A/B was significantly altered using stringent criteria of gene selection. KO lungs displayed a 278-fold decrease in PLUNC mRNA levels (Table S1). PLUNC, which is also referred to as SPLUNC1 or SPURT, is a member of the bactericidal permeability–increasing (BPI) protein/PLUNC superfamily, whose members are thought to have the ability to bind and transfer lipid through their lipid-binding domains (Yamashita et al., 2001; Di et al., 2003; Bingle et al., 2004). The function of PLUNC proteins is unclear, but they are hypothesized to be involved in host defense mechanisms

The graph on the right depicts quantification of Nogo-A/B staining with multiple sections from multiple mice using the scoring system, where 3 is 100% positive staining and 0 is an absence of staining (*, $P < 0.01$). Data are expressed as the mean ± SEM. $n = 4$–8 mice for both groups and data are representative of three experiments. Serial sections were stained with E-cadherin (e and f), H&E (g and h), and PAS (i and j). (C) Representative images of large (a and b) and small (c and d) airways from human lung sections of normal and fatal asthmatic specimens stained for Nogo with the N-18 antibody. Airway epithelium is indicated with arrowheads and vessels with asterisks. Bars: (top) 200 µm; (bottom) 100 µm. Images are representative of four individual normal human lung specimens and one individual fatal asthmatic specimen, with additional patient samples in Fig. S2. (D) Lung sections from control (top) and OVA-treated (bottom) Nogo-$A/B^{+/-}$ LacZ mice stained for β-gal. Airways (both E-cadherin and SMA positive) are indicated with A and vessels (SMA positive only) are indicated with V. Bars, 100 µm. Images represent results obtained from three individual experiments where $n = 6$ mice.

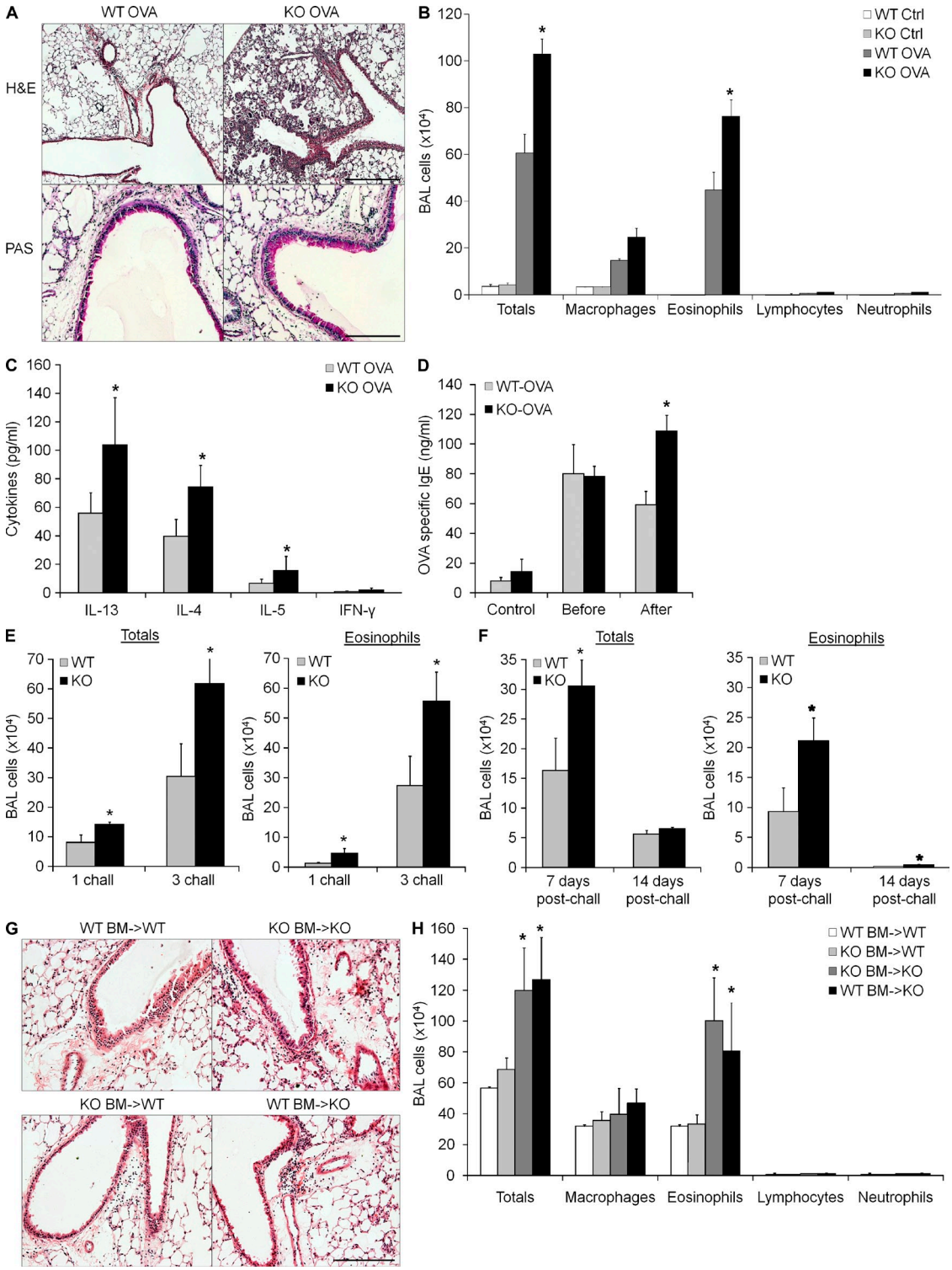

Figure 3. Nogo-A/B KO mice display exaggerated antigen-driven Th2 inflammatory responses. (A) Representative lung sections from allergic WT and Nogo-A/B KO (KO). (B) Total and differential cell counts in BAL fluid from WT and KO control and OVA-challenged mice (*, $P < 0.01$). (C) Levels of Th2 cytokines IL-13, IL-4, and IL-5 and IFN-γ as a Th1 cytokine for control were measured in BAL of WT and KO OVA mice (*, $P < 0.05$). (D) Levels of OVA-specific IgE in serum of WT and KO control mice and in OVA mice before (sensitized only) and after challenge (*, $P = 0.013$). (E) Total cells and eosinophils were measured in BAL of allergic WT and KO mice as described in Results. *, statistically significant from WT mice. (F) 7 and 14 d after 3-d challenge (*, $P < 0.05$). (G and H) Lung histology (G) and cell counts (H) in BAL in OVA-challenged BMT mice (*, $P < 0.05$). Data are expressed as the mean ± SEM. n = 4–8 mice for all groups representative of four individual experiments. Bars, 100 µm.

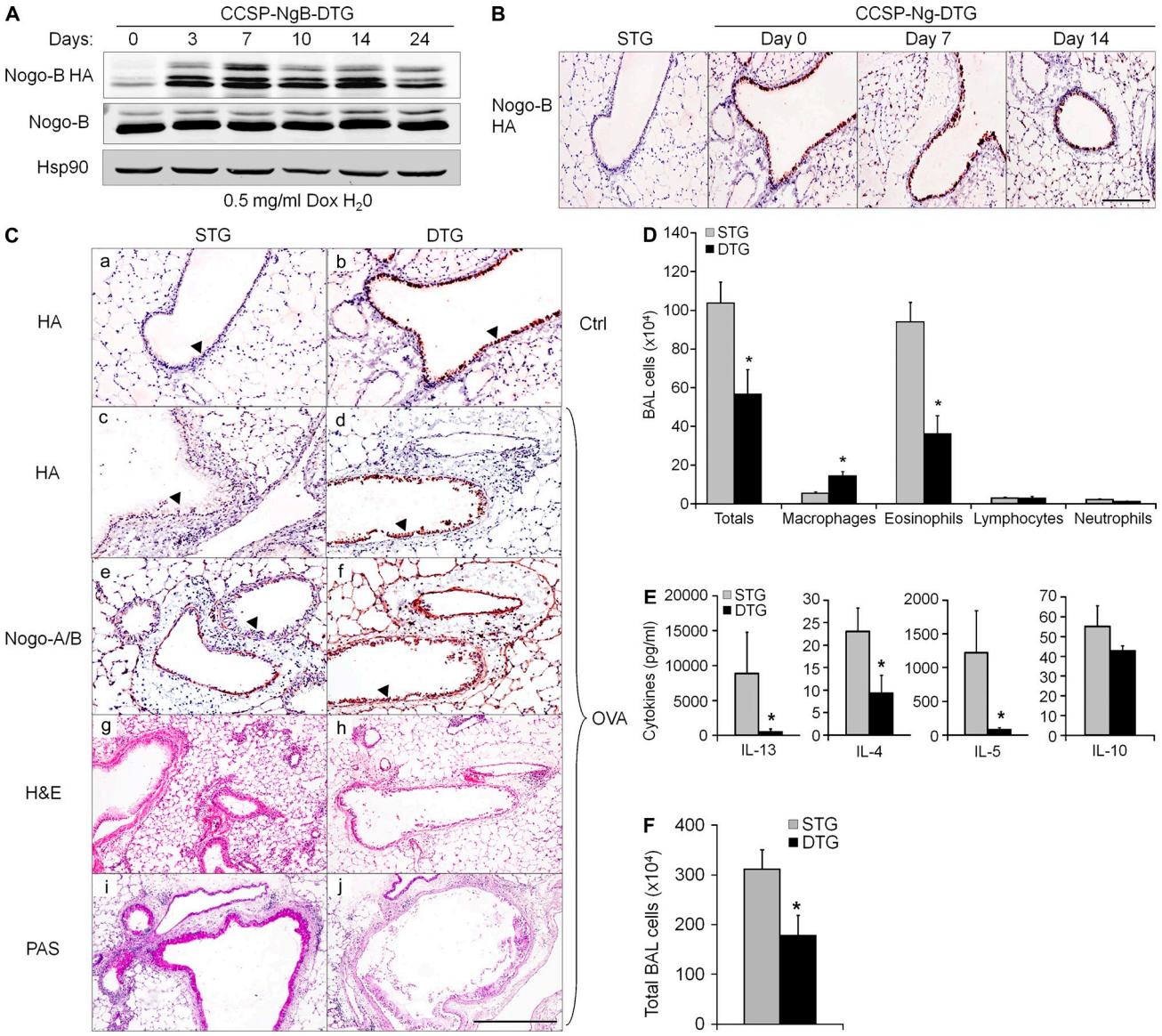

Figure 4. Transgenic expression of Nogo-B in lung epithelium inhibits allergic Th2 inflammation. (A) CCSP-Nogo-DTG mice were put on doxycycline water (0.5 mg/ml) for different time points and the levels of Nogo-B HA–tagged transgene assessed. Endogenous mouse Nogo-B and hsp90 levels were used as loading controls. Each lane represents lung lysate from an individual mouse and was repeated one additional time. (B) Transgene expression in lung sections from CCSP-Ng-DTG mice. Bars, 100 µm. (C) CCSP-Ng-STG and DTG littermates were put on doxycycline water for 7 d before OVA sensitization/challenge. Lung sections from control and OVA-sensitized and challenged STG and DTG mice were stained for transgene expression (a and b, and c and d, respectively), Nogo-A/B (e and f), H&E (g and h), and PAS (I and j). Arrowheads highlight airway epithelium. Bar, 200 µm. (D and E) BAL cell counts (D) and levels of cytokines (E) were evaluated from BAL of OVA STG and DTG mice (*, $P < 0.05$). (F) WT OTII CD4$^+$ Th2 cells were purified and adoptively transferred into STG and DTG mice, followed by OVA challenge and evaluation of total levels of inflammation in the BAL (*, $P < 0.05$). Data are expressed as the mean ± SEM. n = 5–8 mice for both groups representative of three individual experiments.

through their BPI-related N-terminal domain (Sung et al., 2002). Most recently, PLUNC has been shown to exhibit anti-inflammatory functions (Chu et al., 2007). Differences in PLUNC mRNA levels were confirmed by quantitative (q) RT-PCR to be significantly decreased in KO lungs by 95%, whereas two other microarray targets close to significance, TFF2 and Reg3γ, which were decreased by three- and five-fold in KO lungs, respectively, did not display differences by qRT-PCR (Fig. 5 A). As previously reported, PLUNC mRNA levels in tissue were reduced after OVA challenge in WT mice (Chu et al., 2007) and PLUNC gene expression was even further decreased in lungs from OVA-challenged KO mice (Fig. 5 B). The basal reduction of PLUNC protein was also observed in the BAL of KO mice as compared with WT mice (Fig. 5 C), whereas PLUNC levels were increased in naive CCSP-Nogo-B DTG mice compared with STG

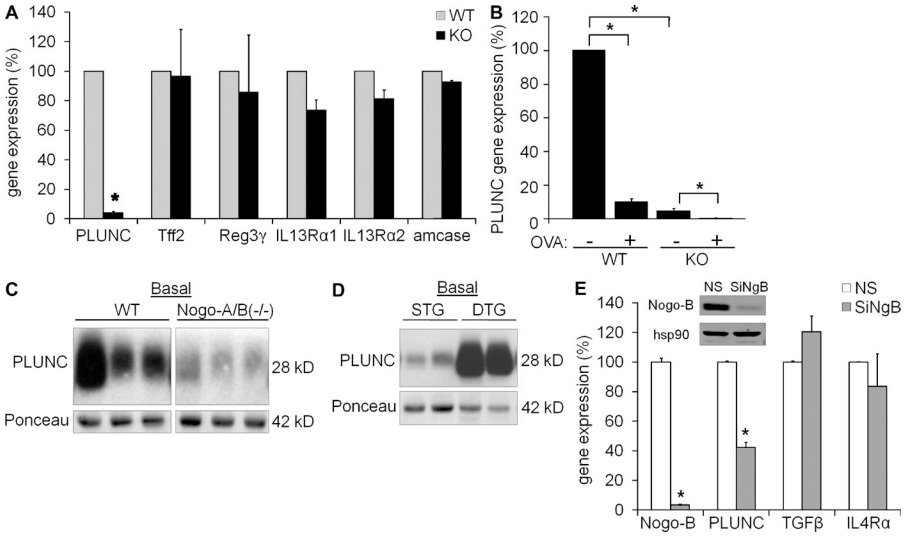

Figure 5. Nogo regulates Plunc expression in vivo and in vitro. (A) Levels of basal gene expression (PLUNC, Tff2, Reg3γ, IL13Rα1, IL13Rα2, and amcase) in WT and Nogo-A/B KO (KO) lungs were determined by qRT-PCR. Data were expressed relative to WT gene expression of 100% (*, $P < 0.01$). (B) PLUNC gene expression in lungs from control and allergic mice. Data are expressed relative to WT control gene expression of 100% (*, $P < 0.01$). (C and D) Basal levels of PLUNC protein were analyzed in BAL of WT and Nogo-A/B$^{-/-}$ mice (C) and in BAL of CCSP-Ng-STG and –DTG mice (D) put on doxycycline water for 3 mo using a PLUNC antibody. Ponceau-stained band at 150 Kb was used as a loading control. (E) NHBECs were treated with a nonsilencing (NS) siRNA or siRNA specifically targeting Nogo-B for 72 h and evaluated for gene expression of Nogo-B, Plunc, TGF-β, and IL4Rα by qRT-PCR. Data were expressed relative to NS gene expression of 100% (*, $P < 0.01$). Data are expressed as the mean ± SEM. n = 3–6 mice for all groups representative of three experiments with each sample run in triplicate.

control mice (Fig. 5 D). To directly link Nogo-B to the expression of PLUNC, Nogo-B levels were reduced in normal human bronchial epithelial cells (NHBECs) using siRNA, and PLUNC mRNA levels were evaluated. As expected, Nogo-B siRNA reduced Nogo protein levels by 80–90% and lowered PLUNC mRNA levels by 60% (Fig. 5 E). The decrease in PLUNC mRNA levels after Nogo-B silencing was specific because the mRNA levels of TGF-β1 and IL-4Rα were unchanged.

The transgenic expression of PLUNC into lung epithelium rescues enhanced asthma-like response in Nogo-A/B$^{-/-}$ mice

CCSP-PLUNC transgenic mice (PTG), which constitutively express the human form of PLUNC specifically in lung epithelium, were generated (unpublished data). PTG mice were then bred onto the Nogo-A/B$^{-/-}$ background to achieve PTG-KO mice and evaluated for transgene expression and localization. Endogenous PLUNC expression was detected exclusively in epithelial cells lining the trachea (Fig. 6 A, top left) and the upper parts of the main bronchi of WT mice, whereas PLUNC was detected to a lesser extent in corresponding lung epithelium of KO mice (Fig. 6 A, top right). These findings are consistent with reduced PLUNC levels in BAL of KO mice (Fig. 6 B). Transgenic PLUNC was present in epithelial cells of the trachea (Fig. 6 A, bottom left) and upper part of the large bronchi as indicated by the enhanced expression of PLUNC staining in PTG and PTG-KO mice. Transgenic PLUNC was also present in epithelium of small airways of PTG and PTG-KO (Fig. 6 A, insets) where endogenous PLUNC is not normally expressed. As seen in Fig. 6 B, transgenic human PLUNC protein expression was detected from endogenous mouse levels as they migrate differently on SDS-PAGE gel and are detected by species-specific antibodies. Transgenic human PLUNC expression runs faster than murine PLUNC on SDS PAGE, is detected at similar levels in the BAL fluid of PTG and PTG-KO mice, and does not change with OVA challenge (Fig. 6 B, compare lanes 3, 4, 7, and 8). As shown before, endogenous mouse PLUNCs are reduced by OVA in WT mice (Fig. 6 B, lanes 2 and 4) and remained greatly reduced in PTG-KO mice compared with PTG. Interestingly, transgenic expression of PLUNC in Nogo KO mice greatly diminished lung inflammation (Fig. 6 C) and total inflammatory cells in their BAL (Fig. 6 D). These data demonstrate that the loss of PLUNC in Nogo-deficient mice may explain, in part, the enhanced lung inflammation in this strain of mice because transgenic rescue of PLUNC normalizes the Nogo KO phenotype.

DISCUSSION

Our results show an unanticipated role of Nogo-B in the lung where it serves a prominent role in the host defense system and controls the extent of Th2-mediated asthma and asthma-like inflammation and disease progression. While exploring potential mechanisms of Nogo function, microarray results identified a single gene markedly down-regulated in lung extracts from Nogo KO mice: PLUNC. Indeed, Nogo regulation of PLUNC gene expression participates in Th2-driven lung inflammation because PLUNC levels in BAL fluid are reduced in Nogo KO mice and elevated in epithelial-specific Nogo-B transgenic mice. Genetic epistasis experiments demonstrate that transgenic reexpression of PLUNC in a Nogo-deficient background partially rescues lung inflammation, demonstrating the causal link between the loss of Nogo and PLUNC and enhanced inflammation.

There are now several studies describing Nogo family members as either negative or positive regulators of disease pathogenesis. In models of nerve regeneration or dysfunction

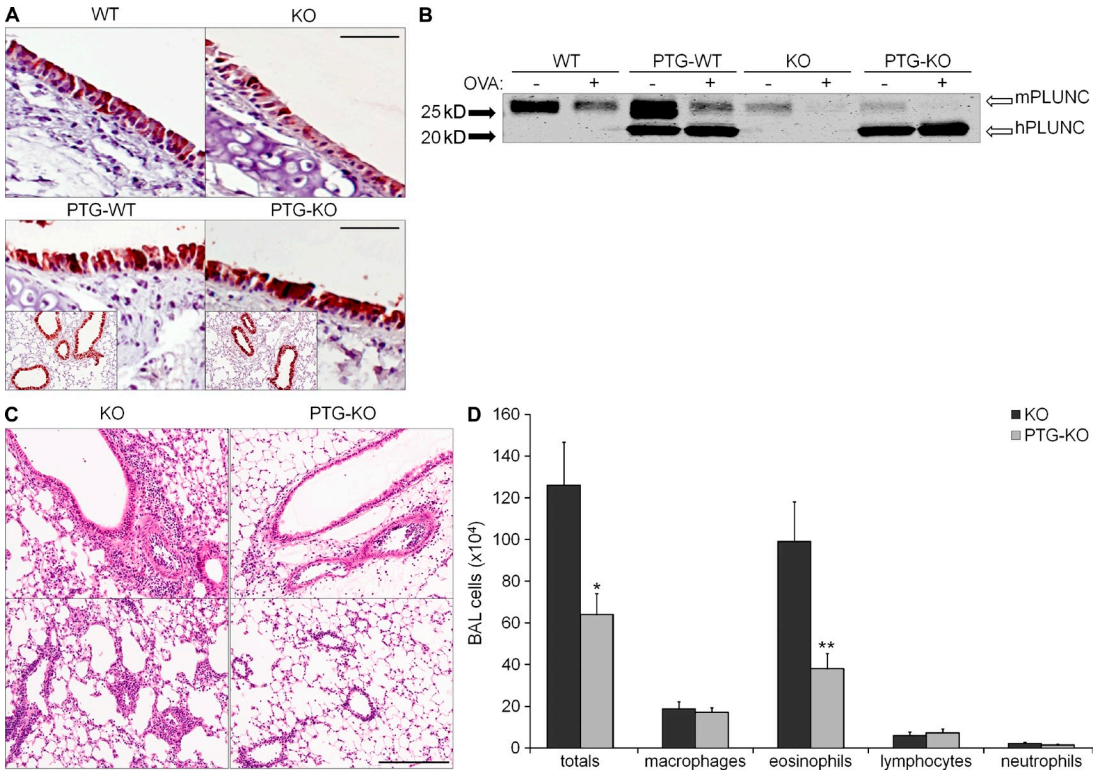

Figure 6. Transgenic expression of PLUNC in lungs of Nogo-A/B KO mice reduces allergic Th2 inflammation. (A) Lung sections from WT, KO, PLUNC transgenic (PTG)–WT, and PTG-KO were stained for PLUNC. Endogenous PLUNC (only in the trachea and upper airways) was observed in tracheal epithelium of WT and, to a lesser extent, in KO (top). Transgenic PLUNC was observed in epithelium of upper airways (bottom) as well as further down the smaller airways (insets) in both WT and KO backgrounds. (B) BAL from WT, PTG-WT, KO, and PTG-KO mice with and without OVA challenge were immunoblotted for levels of endogenous PLUNC (mPLUNC at 25 kD) and transgenic PLUNC (hPLUNC at 20 kD) protein expression. Each lane of the Western blot represents lung lysate from typical individual mouse and was observed in $n = 4–8$ mice for each group. (C and D) Lung H&E staining (C) and total and differential BAL cell counts (D) of KO and PTG-KO mice challenged with OVA (*, $P < 0.05$; **, $P < 0.01$). Bars, 200 µm. Data are expressed as the mean ± SEM. $n = 6$ mice for both groups representative of two experiments.

in the CNS (Yang and Strittmatter, 2007) and after vascular injury (Acevedo et al., 2004; Paszkowiak et al., 2007), Nogo-A and Nogo-B, respectively, may serve independent inhibitory functions and the inhibitory role of Nogo-A appears to be model dependent. In regeneration models, Nogo-A or fragments of Nogo-A are presumably released from damaged myelin to dampens axonal growth. In the vascular injury models, endogenous Nogo-B gene expression is reduced in the inflamed vessel and reintroduction of Nogo-B rescues this phenotype by promoting endothelial cell migration and reduces smooth muscle cell proliferation and migration (Acevedo et al., 2004; Kritz et al., 2008). However, in models of wound healing and tissue ischemia, endogenous Nogo-B participates in the extent of recovery, largely via regulation of macrophage motility and gene expression (Yu et al., 2009). Thus, it appears that Nogo isoforms exert diverse actions in multiple cell types, and the differences in function are likely attributable to the intracellular role of the RTN domain versus the biologically active fragments generated upon tissue damage. Clearly, in the model of Th2 lung inflammation in the present study, Nogo-B exerts cell restricted actions within the epithelium. During the evolution of Th2 inflammation, Nogo-B expression decreases in airway epithelium and smooth muscle yet increases in the pulmonary vasculature. These cell type–specific changes of Nogo gene expression are most likely a result of local factors (inflammatory cytokines, particularly the Th2 cytokines IL-13 and IL-4) in the asthmatic-like milieu. In addition, the genetic loss of Nogo enhances the magnitude of Th2-driven allergic inflammation, in part by controlling the expression of the airway epithelial antiinflammatory protein PLUNC. Therefore, the importance or relevance of changes in Nogo expression in certain cell types may depend on the disease environment and nature of the inflammatory response. Although Nogo-B is ubiquitously expressed, the differential regulation of Nogo expression in alternate cell types highlights the idea that Nogo may exert varying functions in each cell type even within the same disease paradigm. With respect to how the Nogo gene is regulated, there has been a single extensive study on the Nogo-A/B promoter (Oertle et al., 2003); however, the regulation of Nogo expression in individual cells types has not yet been systematically evaluated. Whether the changes in Nogo-B expression are consequences of the asthmatic-like response or causal to disease progression is not entirely clear. Yet, when Nogo-B is reconstituted back

into the lung epithelium using tissue-specific transgenic mice, this is sufficient to reduce Th2-driven inflammation. This suggests that the loss of Nogo in the epithelium during asthma pathogenesis contributes to this disease. The importance of cell specificity of Nogo-B function is exemplified by the lack of effect of endothelial Nogo-B expression on the asthmatic-like response.

One aspect of murine asthma-like responses that have been extensively studied is the importance of $CD4^+$ Th2 cells and cytokines, which is a hallmark of asthma pathogenesis (Cohn et al., 2004). Although Nogo-B is found in inflammatory cells (Yu et al., 2009), BMT experiments clearly show that the major role for Nogo-B exists in the tissue and not the BM-derived cells. OVA-specific IgE levels were similar in WT and Nogo KO mice after sensitization, implying that loss of Nogo-A/B does not alter the sensitization process, development of antigen-specific memory responses, and IgE class switching. It is only after aerosolized OVA challenge that a difference in OVA-specific IgE is detected in Nogo KO mice, supporting the idea that Nogo-B regulates aspects of the effector phase but not priming/sensitization phases of the asthmatic response. Upon further dissection of the time course of inflammation in Nogo KO mice, enhanced Th2 lung inflammation occurs as early as 24 h after allergen challenge. Therefore, Nogo-B inhibitory function is involved in the very early phase of Th2-mediated lung inflammation, and without it the environment is staged for an enhanced and prolonged inflammatory response. This is evident in Nogo KOs, which display increased lung inflammation 7 d after challenge and residual eosinophils even 14 d after challenge.

It is apparent that the airway epithelium plays a major role in the phenotype observed in Nogo KO mice. The airway epithelium functions not only as a protective barrier but also orchestrates aspects of the inflammatory response including the production of chemokines (Holgate, 2007). Using an unbiased microarray approach to monitor gene expression in lungs from naive WT and Nogo KO mice reveals a remarkable decrease in PLUNC gene expression, a result confirmed at the protein level in vivo. PLUNC has recently been described as an antibacterial antiinflammatory protein that is specifically expressed and secreted by epithelial cells of the upper airways and nasal cavity (Chu et al., 2007). Therefore, Nogo KO mice, which express low levels of PLUNC, may have impaired airway barrier protection causing these mice to become more susceptible to lung insults such as allergic Th2 inflammation. Any compromise of epithelial integrity can create a vulnerability to inhaled substances and susceptibility to activation of inflammatory responses (Holgate, 2007). Thus, the role for Nogo in the airway epithelium could certainly be expanded to other diseases of the lung that are generated through this route of entry.

Exactly how Nogo regulates PLUNC gene expression is not yet known; however, there is a direct correlation between Nogo levels and PLUNC expression and this coincides with the extent of lung inflammation. Evidence for a causal link between these genes are experiments showing that the genetic loss or gain of Nogo function in the epithelium in vivo regulates PLUNC levels and, more directly, siRNA-mediated reduction of Nogo-B in cultured epithelial cells also reduces PLUNC mRNA levels, recapitulating the microarray dataset. Interestingly, these in vitro experiments require the intracellular function of Nogo in ER (Voeltz et al., 2006; Shibata et al., 2008), and perhaps by maintaining the integrity of the reticular ER Nogo-B regulates aspects of ER stress and/or transcriptional control of the PLUNC gene. It is appreciated that ER stress is a component of asthma and other chronic inflammatory diseases (Cantero-Recasens et al., 2010), and the contemporaneous regulation of PLUNC by Nogo-B is striking and a novel area of exploration.

Thus, Nogo-B in the lung serves a major role in the airway epithelium as an inhibitor of antigen-driven Th2 inflammation as supported by genetic loss and gain of function approaches. Further elucidation of the mechanisms underlying the interplay between Nogo and PLUNC affords new insights into the complex role of RTNs and offers great potential for revealing opportunities for therapeutics that modulate the inflammatory response in a range of diseases.

MATERIALS AND METHODS

Mice

Nogo-A/B$^{-/-}$ and Nogo-A/B$^{-/-}$ LacZ mice. Nogo-A/B$^{-/-}$ mice were provided by M. Tessier-Levigne (Genentech, South San Francisco, CA; Zheng et al., 2003). Nogo-A/B$^{-/-}$ LacZ gene reporter mice were provided by S, Strittmatter (Yale University, New Haven, CT; Kim et al., 2003). Both strains were crossed onto a C57BL6 background for >10 generations and used at 6–8 wk of age for these studies.

CCSP-Nogo-B transgenic mice. A transgene encoding ptet-splice-TRE (tetracycline responsive element), followed by HA-tagged human Nogo-B, was used to generate NogoB TG reporter mice. These mice were bred to lung epithelial CCSP driver mice (J. Whitsett, Cincinnati Children's Hospital Medical Center, Cincinnati, OH; Tichelaar et al., 2000), which use the Clara cell 10-kD protein (CC10) promoter to express the reverse tetracycline transactivator using a Tet-On system to achieve DTG positive for both CCSP and NogoB TG mice (DTG) and single transgenic positive for either CCSP or NogoB TG mice (STG). Mice were bred onto a C57BL/6 background for >10 generations, and littermates were used in these studies.

CCSP-PLUNC transgenic Nogo-A/B$^{-/-}$ mice. CCSP-PLUNC transgenic positive mice (PTG; P. Di, University of Pittsburgh, Pittsburgh, PA) contain the transgenes for the CC10 promoter driver and the human PLUNC gene for constitutive expression in Clara cells. PTG mice were bred to Nogo-A/B KO mice to obtain PTG-KO mice and littermate KO mice were used as controls.

Doxycycline water administration. 6-wk-old DTG mice and STG littermate controls were given 0.5 mg/ml doxycycline in their drinking water for 2 wk before experiments were conducted as previously described (Ray et al., 1997; Fontoura et al., 2004). All animal experiments were approved by the Yale School of Medicine Institutional Animal Care and Use Committee in accordance with federal guidelines.

OVA/Alum sensitization and challenge

OVA sensitization and challenge was accomplished using modifications of the protocols previously described by Wang et al. (2000). In brief, mice 6–8 wk of age were immunized with 10 μg of chicken OVA fraction V (Sigma-Aldrich) in a 2% ALUM suspension by i.p. injection on days 0 and 5. On days 12, 13, and 14, mice were challenged for 30 min with an aerosol of 1% OVA

in endotoxin-free PBS using a compressor nebulizer (Comp Air Elite NE-C21V; OMRON). Mice were sacrificed 24 h after the last challenge. Control mice were given PBS in place of OVA in the i.p. sensitization and/or challenge stages of the protocol.

Adoptive transfer of OTII CD4+ Th2 cells

CD4 T cells from OT-II mice transgenic for OVA-specific TCR were isolated and polarized in vitro to TH2 cells as previously described by our laboratories (Niu et al., 2007). Cultured Th2-like cells were harvested after 4 d and 2×10^6 cells were injected i.v. into syngeneic recipients. 1 d after transfer of cells, mice were challenged with 1% OVA aerosol in endotoxin-free PBS for a total of 7 d and sacrificed 24 h after the last challenge.

Tissue isolation and histology

As described previously by our laboratories (Wang et al., 2000), animals were anesthetized, a median sternotomy was performed, and right heart perfusion was accomplished with calcium and magnesium-free PBS. The right lung was either collected immediately for protein or RNA isolation or frozen in liquid nitrogen and stored at −80°C until later use. The heart and lungs were removed en bloc, inflated at 25-cm pressure with 0.5% low melting point agarose, fixed, paraffin embedded, sectioned, and stained. Stains for hematoxylin and eosin (H&E) and PAS for mucus were performed by the Research Histology Laboratory, Department of Pathology, at the Yale University School of Medicine.

Human lung tissue specimens

Five human lung tissue samples were obtained under the guidance of Dr. Robert Homer from the Yale Center for Asthma and Airways Disease tissue bank. Four of these tissue specimens considered to be nonasthmatic were acquired from excess tissue resected during surgical procedures. One individual tissue sample was acquired from lung tissue of a fatal asthmatic. All specimens were paraffin embedded and tissue processed using standard clinical techniques by Yale Pathology guidelines. Sections were cut at 5-µm thickness onto positively charged slides.

Immunohistochemistry

For immunodetection of proteins, sections were rehydrated, blocked with 3% H_2O_2, and antigen retrieval was performed. Sections were blocked and permeabilized in 10% donkey serum, 0.5% BSA, and 0.1% Triton X-100. Primary antibodies used were: α-SMA (Dako), high-affinity HA antibody (Roche), E-cadherin (Invitrogen), Nogo-A/B using Nogo1761 antibody serum designed by our laboratory against aa 17–61 (Imgenex), and biotin-conjugated human PLUNC antibody (R&D Systems). Secondary antibodies included biotin-conjugated anti–rabbit, –mouse, and –goat (Jackson Immunoresearch Laboratories). Counterstaining was performed using Mayer's hematoxylin. Images were taken with a light microscope (Eclipse 80i; Nikon). Nogo-A/B staining was quantified using a scoring system, where 3 was 100% staining and 0 was an absence of staining as determined by a blinded observer.

X-gal staining

Lungs were fixed in buffer (1% formalin, 0.002% glutaraldehyde, and 0.0002% NP-40 in PBS, pH 7.4–7.6) for 10 min at room temperature. Lungs were stained with X-gal buffer (1 mg/ml X-gal in DMSO [American Bioanalytical], 5 mM K-ferricyanide, 5 mM K-ferrocyanide, 2 mM $MgCl_2$, and 0.02% NP-40) and developed at 37°C overnight. WT lungs were treated equivalently as control. Lungs were paraffin embedded and cut in 10-µm sections. Slides were deparaffinized, rehydrated, and counterstained with nuclear fast red (TACS). Images were taken with a light microscope.

Protein isolation and immunoblot analysis

Proteins from lung tissue and cell lysates were resolved by SDS/PAGE and immunoblotting as described previously by our laboratory (Suárez et al., 2008). Primary antibodies used were Nogo1761 antibody, as described in Immunohistochemistry, Hsp90 (Santa Cruz Biotechnology, Inc.), and biotinylated mouse and human PLUNC antibodies (R&D Systems). Secondary antibodies were fluorophore conjugated (LI-COR Biosciences). Bands were visualized using the Odyssey Infrared Imaging System (LI-COR Biosciences).

BAL

Lung inflammation was assessed in BAL as described previously with slight modification (Wang et al., 2000; Kang et al., 2007). In brief, trachea was cannulated and lung was lavaged twice with 0.8 ml PBS, pooled, and centrifuged for each animal. Supernatant was stored at −80°C for later analysis of cytokines by ELISA. Pelleted cells were evaluated for total cell counts using a hemacytometer. For differentials, 5×10^4 cells were aliquoted for cytospin and spun at 14,000 rpm for 5 min and stained with Diff-Quick (Thermo Fisher Scientific). The number and type of cells in the cell pellet were determined with light microscopy.

Cytokine detection assays

Cytokine levels were analyzed from BAL by ELISA (R&D Systems) for IL-13, IL-4, IL-5, and IFN-γ.

IgE

Blood was collected by eye bleeds before OVA challenge and by cardiac puncture for after OVA challenge. Blood clots were removed and blood was spun down to separate serum. Serum levels of total and OVA-specific IgE were determined by ELISA, as per the manufacturer's instructions.

BMT

BMTs were conducted as previously reported by our laboratory (Fernández-Hernando et al., 2007). In brief, Nogo-A/B KO or WT mice 6–8 wk old were lethally irradiated with 1,000 rads (10 Gy) from a cesium source 4 h before transplantation. BM was collected from femurs of donor Nogo-A/B KO or WT mice by flushing with sterile medium (RPMI 1640, 2% FBS, 5 U/ml heparin, 50 U/ml penicillin, and 50 mg/ml streptomycin). Recipient mice were injected with 2×10^6 BM cells through the jugular vein. 4 wk after BMT, peripheral blood was collected for PCR analysis of BM reconstitution. 8 wk after BMT, mice were fully chimeric and subjected to OVA model of asthma.

Microarray

Whole lung tissue RNA from 8-wk-old naive WT and Nogo-A/B KO mice (Genentech) was isolated using a hybrid Trizol/QIAGEN protocol of RNA isolation. High purity of RNA was confirmed by spectrophotometric measurements and RNA agarose gel electrophoresis. RNA samples from three biological replicates of each group were hybridized to whole genome mouse arrays (Agilent Technologies). Sample preparation, labeling, and array hybridizations were performed according to standard protocols from the University of California, San Francisco Shared Microarray Core Facilities and Agilent Technologies. A linear model was fit to the comparison to estimate the mean M values and calculated moderated t statistic, B statistic, false discovery rate, and p-value for each gene for the comparison of interest. Adjusted p-values were produced by the method proposed by Holm (1979). All procedures were performed using functions in the R package *limma in Bioconductor* (Gentleman et al., 2004).

qRT-PCR

Total RNA was extracted from homogenized lungs using Trizol (Invitrogen), followed by further purification with RNeasy columns (QIAGEN). Reverse transcription was performed on RNA using the TaqMan reverse transcription kit (Applied Biosystems). Equal amounts of cDNA were prepared with Sybr Green MasterMix (Bio-Rad Laboratories) and primers designed for genes of interest and run on an iCycler machine (Bio-Rad Laboratories). Data were normalized to 18s levels and expressed relative to control.

NHBEC cultures and siRNA treatment

NHBECs (Lonza) were cultured according to manufacturer's instructions. At 60% confluency, cells were treated with siRNA nonsilencing control (QIAGEN) or siRNA against human Nogo-B gene (QIAGEN) precomplexed

wtih oligofectamine (1 µl per pmol of siRNA; Invitrogen) at 37°C. After 6 h, cells were supplemented with 2× media and further treated with siRNA (final concentration of 40 nM) for 72 h.

Statistics

Normally distributed data are expressed as SEM and assessed for significance between groups by two-tailed Student's *t* test or two-way ANOVA with Bonferroni correction for multiple comparisons when appropriate. Values of $P < 0.05$ were considered statistically significant and are representative of evaluations in a minimum of six mice.

Pulmonary function test

The baseline resistance and AHR in unrestrained conscious animals were assessed by barometric plethysmography using whole-body plethysmography (Buxco Electronics) as described by our laboratory (Zhu et al., 1999). In brief, mice were placed into whole-body plethysmographs and interfaced with computers using differential pressure transducers. Measurements were made of respiratory rate, tidal volume, and enhanced pause. Airways resistance is expressed as $P_{enh} = [(t_e/0.3\ t_r) - 1] \times (2\ P_{ef}/3\ P_{if})$, where P_{enh} = enhanced pause, t_e = expiratory time (in seconds), t_r = relaxation time (in seconds), P_{ef} = peak expiratory flow (in milliliters), and P_{if} = peak inspiratory flow (in milliliters per second). Increasing doses of methacholine were administered by nebulization for 2 min, and P_{enh} was calculated over the subsequent 5 min.

OVA/CFA sensitization and challenge

OVA sensitization and challenge was accomplished using modifications of the protocols as previously described (Cohn et al., 1997; Yip et al., 1999). In brief, mice 6–8 wk of age were immunized with an emulsion of chicken OVA fraction V (10 µg; Sigma-Aldrich) in CFA by s.c. injection along each flank on day 0. On days 12, 13, and 14, mice were challenged for 30 min with an aerosol of 1% OVA in endotoxin-free PBS using a compressor nebulizer (Comp Air Elite NE-C21V). Mice were sacrificed 24 h after the last challenge. Control mice were given PBS in place of OVA in the i.p. sensitization and/or challenge stages of the protocol.

Online supplemental material

Fig. S1 demonstrates that Nogo-A is undetectable in lysates prepared from naive or sensitized and challenged lungs. Fig. S2 shows the loss of immunoreactive Nogo-B in lung sections from three additional fatal asthmatic specimens. Fig. S3 depicts increased airway hyperreactivity in sensitized and challenged Nogo-A/B KO mice compared with littermate controls. Fig. S4 documents that Th1-driven lung inflammation in Nogo-A/B KO mice does not differ from control mice. Online supplemental material is available at http://www.jem.org/cgi/content/full/jem.20100786/DC1.

We would like to acknowledge the Sandler Asthma Basic Research Center Functional Genomics Core Facility for assistance with microarray studies.

This work was supported by grants R01 HL64793, R01 HL61371, R01 HL081190, R01 HL096670, and P01 HL70295, and a Senior Investigator Award from the American Asthma Foundation to W.C. Sessa.

The authors have no competing financial interests.

Submitted: 21 April 2010
Accepted: 29 September 2010

REFERENCES

Acevedo, L., J. Yu, H. Erdjument-Bromage, R.Q. Miao, J.E. Kim, D. Fulton, P. Tempst, S.M. Strittmatter, and W.C. Sessa. 2004. A new role for Nogo as a regulator of vascular remodeling. *Nat. Med.* 10:382–388. doi:10.1038/nm1020

Bingle, C.D., E.E. LeClair, S. Havard, L. Bingle, P. Gillingham, and C.J. Craven. 2004. Phylogenetic and evolutionary analysis of the PLUNC gene family. *Protein Sci.* 13:422–430. doi:10.1110/ps.03332704

Cantero-Recasens, G., C. Fandos, F. Rubio-Moscardo, M.A. Valverde, and R. Vicente. 2010. The asthma-associated ORMDL3 gene product regulates endoplasmic reticulum-mediated calcium signaling and cellular stress. *Hum. Mol. Genet.* 19:111–121. doi:10.1093/hmg/ddp471

Chen, M.S., A.B. Huber, M.E. van der Haar, M. Frank, L. Schnell, A.A. Spillmann, F. Christ, and M.E. Schwab. 2000. Nogo-A is a myelin-associated neurite outgrowth inhibitor and an antigen for monoclonal antibody IN-1. *Nature.* 403:434–439. doi:10.1038/35000219

Chu, H.W., J. Thaikoottathil, J.G. Rino, G. Zhang, Q. Wu, T. Moss, Y. Refaeli, R. Bowler, S.E. Wenzel, Z. Chen, et al. 2007. Function and regulation of SPLUNC1 protein in Mycoplasma infection and allergic inflammation. *J. Immunol.* 179:3995–4002.

Cohn, L., R.J. Homer, A. Marinov, J. Rankin, and K. Bottomly. 1997. Induction of airway mucus production By T helper 2 (Th2) cells: a critical role for interleukin 4 in cell recruitment but not mucus production. *J. Exp. Med.* 186:1737–1747. doi:10.1084/jem.186.10.1737

Cohn, L., J.A. Elias, and G.L. Chupp. 2004. Asthma: mechanisms of disease persistence and progression. *Annu. Rev. Immunol.* 22:789–815. doi:10.1146/annurev.immunol.22.012703.104716

Di, Y.P., R. Harper, Y. Zhao, N. Pahlavan, W. Finkbeiner, and R. Wu. 2003. Molecular cloning and characterization of spurt, a human novel gene that is retinoic acid-inducible and encodes a secretory protein specific in upper respiratory tracts. *J. Biol. Chem.* 278:1165–1173. doi:10.1074/jbc.M210523200

Fernández-Hernando, C., E. Ackah, J. Yu, Y. Suárez, T. Murata, Y. Iwakiri, J. Prendergast, R.Q. Miao, M.J. Birnbaum, and W.C. Sessa. 2007. Loss of Akt1 leads to severe atherosclerosis and occlusive coronary artery disease. *Cell Metab.* 6:446–457. doi:10.1016/j.cmet.2007.10.007

Fontoura, P., P.P. Ho, J. DeVoss, B. Zheng, B.J. Lee, B.A. Kidd, H. Garren, R.A. Sobel, W.H. Robinson, M. Tessier-Lavigne, and L. Steinman. 2004. Immunity to the extracellular domain of Nogo-A modulates experimental autoimmune encephalomyelitis. *J. Immunol.* 173:6981–6992.

Gentleman, R.C., V.J. Carey, D.M. Bates, B. Bolstad, M. Dettling, S. Dudoit, B. Ellis, L. Gautier, Y. Ge, J. Gentry, et al. 2004. Bioconductor: open software development for computational biology and bioinformatics. *Genome Biol.* 5:R80. doi:10.1186/gb-2004-5-10-r80

GrandPré, T., F. Nakamura, T. Vartanian, and S.M. Strittmatter. 2000. Identification of the Nogo inhibitor of axon regeneration as a Reticulon protein. *Nature.* 403:439–444. doi:10.1038/35000226

Holgate, S.T. 2007. Epithelium dysfunction in asthma. *J. Allergy Clin. Immunol.* 120:1233–1244, quiz :1245–1246. doi:10.1016/j.jaci.2007.10.025

Holm, S. 1979. A simple sequentially rejective multiple test procedure. *Scandinavian Journal of Statistics.* 6:65–70.

Kang, H.R., C.G. Lee, R.J. Homer, and J.A. Elias. 2007. Semaphorin 7A plays a critical role in TGF-β1–induced pulmonary fibrosis. *J. Exp. Med.* 204:1083–1093. doi:10.1084/jem.20061273

Kim, J.E., S. Li, T. GrandPré, D. Qiu, and S.M. Strittmatter. 2003. Axon regeneration in young adult mice lacking Nogo-A/B. *Neuron.* 38:187–199. doi:10.1016/S0896-6273(03)00147-8

Kritz, A.B., J. Yu, P.L. Wright, S. Wan, S.J. George, C. Halliday, N. Kang, W.C. Sessa, and A.H. Baker. 2008. In vivo modulation of Nogo-B attenuates neointima formation. *Mol. Ther.* 16:1798–1804. doi:10.1038/mt.2008.188

Niu, N., M.K. Le Goff, F. Li, M. Rahman, R.J. Homer, and L. Cohn. 2007. A novel pathway that regulates inflammatory disease in the respiratory tract. *J. Immunol.* 178:3846–3855.

Oertle, T., and M.E. Schwab. 2003. Nogo and its paRTNers. *Trends Cell Biol.* 13:187–194. doi:10.1016/S0962-8924(03)00035-7

Oertle, T., C. Huber, H. van der Putten, and M.E. Schwab. 2003. Genomic structure and functional characterisation of the promoters of human and mouse nogo/rtn4. *J. Mol. Biol.* 325:299–323. doi:10.1016/S0022-2836(02)01179-8

Pan, J.W., M. Wei, P.Y. Yang, X. Zheng, J.B. Li, Z.G. Lu, X.X. Zhao, H. Wu, H. Kang, and Y.C. Rui. 2007. Regulation of Nogo-B expression in the lesion of aortic aneurysms. *Clin. Exp. Pharmacol. Physiol.* 34:856–860. doi:10.1111/j.1440-1681.2007.04673.x

Paszkowiak, J.J., S.P. Maloney, F.A. Kudo, A. Muto, D. Teso, R.C. Rutland, T.S. Westvik, J.M. Pimiento, G. Tellides, W.C. Sessa, and A. Dardik. 2007. Evidence supporting changes in Nogo-B levels as a marker of neointimal expansion but not adaptive arterial remodeling. *Vascul. Pharmacol.* 46:293–301. doi:10.1016/j.vph.2006.11.003

Prinjha, R., S.E. Moore, M. Vinson, S. Blake, R. Morrow, G. Christie, D. Michalovich, D.L. Simmons, and F.S. Walsh. 2000. Inhibitor of neurite outgrowth in humans. *Nature.* 403:383–384. doi:10.1038/35000287

Ray, P., W. Tang, P. Wang, R. Homer, C. Kuhn III, R.A. Flavell, and J.A. Elias. 1997. Regulated overexpression of interleukin 11 in the lung. Use to dissociate development-dependent and -independent phenotypes. *J. Clin. Invest.* 100:2501–2511. doi:10.1172/JCI119792

Rodriguez-Feo, J.A., W.E. Hellings, B.A. Verhoeven, F.L. Moll, D.P. de Kleijn, J. Prendergast, Y. Gao, Y. van der Graaf, G. Tellides, W.C. Sessa, and G. Pasterkamp. 2007. Low levels of Nogo-B in human carotid atherosclerotic plaques are associated with an atheromatous phenotype, restenosis, and stenosis severity. *Arterioscler. Thromb. Vasc. Biol.* 27:1354–1360. doi:10.1161/ATVBAHA.107.140913

Shibata, Y., C. Voss, J.M. Rist, J. Hu, T.A. Rapoport, W.A. Prinz, and G.K. Voeltz. 2008. The reticulon and DP1/Yop1p proteins form immobile oligomers in the tubular endoplasmic reticulum. *J. Biol. Chem.* 283:18892–18904. doi:10.1074/jbc.M800986200

Suárez, Y., C. Fernández-Hernando, J. Yu, S.A. Gerber, K.D. Harrison, J.S. Pober, M.L. Iruela-Arispe, M. Merkenschlager, and W.C. Sessa. 2008. Dicer-dependent endothelial microRNAs are necessary for postnatal angiogenesis. *Proc. Natl. Acad. Sci. USA.* 105:14082–14087. doi:10.1073/pnas.0804597105

Sung, Y.K., C. Moon, J.Y. Yoo, C. Moon, D. Pearse, J. Pevsner, and G.V. Ronnett. 2002. Plunc, a member of the secretory gland protein family, is up-regulated in nasal respiratory epithelium after olfactory bulbectomy. *J. Biol. Chem.* 277:12762–12769. doi:10.1074/jbc.M106208200

Teng, F.Y., and B.L. Tang. 2008. Cell autonomous function of Nogo and reticulons: The emerging story at the endoplasmic reticulum. *J. Cell. Physiol.* 216:303–308. doi:10.1002/jcp.21434

Tichelaar, J.W., W. Lu, and J.A. Whitsett. 2000. Conditional expression of fibroblast growth factor-7 in the developing and mature lung. *J. Biol. Chem.* 275:11858–11864. doi:10.1074/jbc.275.16.11858

Voeltz, G.K., W.A. Prinz, Y. Shibata, J.M. Rist, and T.A. Rapoport. 2006. A class of membrane proteins shaping the tubular endoplasmic reticulum. *Cell.* 124:573–586. doi:10.1016/j.cell.2005.11.047

Wang, J., R.J. Homer, Q. Chen, and J.A. Elias. 2000. Endogenous and exogenous IL-6 inhibit aeroallergen-induced Th2 inflammation. *J. Immunol.* 165:4051–4061.

Woolf, C.J. 2003. No Nogo: now where to go? *Neuron.* 38:153–156. doi:10.1016/S0896-6273(03)00233-2

Yamashita, S., N. Sakai, K. Hirano, M. Ishigami, T. Maruyama, N. Nakajima, and Y. Matsuzawa. 2001. Roles of plasma lipid transfer proteins in reverse cholesterol transport. *Front. Biosci.* 6:D366–D387. doi:10.2741/Yamashita

Yang, Y.S., and S.M. Strittmatter. 2007. The reticulons: a family of proteins with diverse functions. *Genome Biol.* 8:234. doi:10.1186/gb-2007-8-12-234

Yip, H.C., A.Y. Karulin, M. Tary-Lehmann, M.D. Hesse, H. Radeke, P.S. Heeger, R.P. Trezza, F.P. Heinzel, T. Forsthuber, and P.V. Lehmann. 1999. Adjuvant-guided type-1 and type-2 immunity: infectious/noninfectious dichotomy defines the class of response. *J. Immunol.* 162:3942–3949.

Yu, J., C. Fernández-Hernando, Y. Suarez, M. Schleicher, Z. Hao, P.L. Wright, A. DiLorenzo, T.R. Kyriakides, and W.C. Sessa. 2009. Reticulon 4B (Nogo-B) is necessary for macrophage infiltration and tissue repair. *Proc. Natl. Acad. Sci. USA.* 106:17511–17516. doi:10.1073/pnas.0907359106

Zheng, B., C. Ho, S. Li, H. Keirstead, O. Steward, and M. Tessier-Lavigne. 2003. Lack of enhanced spinal regeneration in Nogo-deficient mice. *Neuron.* 38:213–224. doi:10.1016/S0896-6273(03)00225-3

Zhu, Z., R.J. Homer, Z. Wang, Q. Chen, G.P. Geba, J. Wang, Y. Zhang, and J.A. Elias. 1999. Pulmonary expression of interleukin-13 causes inflammation, mucus hypersecretion, subepithelial fibrosis, physiologic abnormalities, and eotaxin production. *J. Clin. Invest.* 103:779–788. doi:10.1172/JCI5909